# Takagi-Sugeno Fuzzy Fault Detector Design with Finite-Frequency Specifications for Autonomous Ground Vehicles

Shengxiang Wang, Jun-Tao Pan, Tran Anh-Tu Nguyen, Thierry-Marie Guerra, Jimmy Lauber

Available online at www.sciencedirect.com

ScienceDirect

IFAC PapersOnLine 54-4 (2021) 195–200

# Takagi-Sugeno Fuzzy Fault Detector Design with Finite-Frequency Specifications for Autonomous Ground Vehicles ⋆

**Sujun Wang** * **Juntao Pan** * **Anh-Tu Nguyen** **,*** **Thierry-Marie Guerra** ** **Jimmy Lauber** **,***

* *School of Electrical and Information Engineering, North Minzu University, Yinchuan, China.*
** *Laboratory LAMIH-CNRS, UMR 8201, Université Polytechnique Hauts-de-France, F-59313 Valenciennes, France.*
*** *INSA Hauts-de-France, F-59313 Valenciennes, France.*
*Email: nguyen.trananhtu@gmail.com, jtpan@aliyun.com.*

**Abstract:** This paper investigates the steering fault detection problem for autonomous ground vehicles (AGVs). Using an observer-based approach, a new fuzzy fault detector for steering actuator is designed for safety concern. To this end, a two degrees-of-freedom (2-DOF) nonlinear vehicle model is adopted to represent the nonlinear dynamics of AGVs. Since it is not easy to measure the lateral velocity in practice, this model is then represented in a specific Takagi-Sugeno (TS) fuzzy form with nonlinear consequents. In contrast to the conventional TS fuzzy modeling, it allows separating the unmeasured premise variables in the local nonlinear consequent, which enables a more effective way to deal with the challenging issue of unmeasured premise variables. Moreover, to minimize the effect of disturbances on system performance and maximize that of actuator faults on the generated residual, both $H_\infty$ disturbance attenuation index and $H_-$ fault sensitivity index are taken into account in a finite-frequency domain. The conditions to design fault detection TS fuzzy observer are derived using Lyapunov stability method. The design procedure can be reformulated as an optimization problem under linear matrix inequalities, efficiently solved by standard numerical solvers. Simulation results are given to verify the fault detection performance of the proposed method.



*Keywords:* Takagi-Sugeno fuzzy models, autonomous vehicles, fault detection, nonlinear observer, unmeasured premise variables, Lyapunov method.

## 1. INTRODUCTION

Real-time information on the vehicle dynamics and deriver-related variables is essential for the active safety issues of autonomous ground vehicles (AGVs). Unfortunately, such information is not always precisely measured by the onboard vehicle sensors due to cost reasons. Moreover, the actuator motions of AGVs, such as steering motions, are realized by electric connection which is not as reliable as traditional mechanical connection. Therefore, the fault detection and fault diagnosis are two critical topics for AGVs (Arogeti et al., 2012; Fang et al., 2020; Li et al., 2021).

Model-based method has been shown as one of the most effective ways deal with fault detection problem for AGVs. The primary principle of model-based fault detection is to evaluate a residual signal generated by the measured signal and the observer output. Since the detection is implemented in a software form, the model-based fault detection has attracted a lot of attentions (Fang et al., 2020). This paper investigates a Takagi-Sugeno (TS) fuzzy model-based approach (Tanaka and Wang, 2004; Nguyen et al., 2019) to design a actuator fault detector for AGVs. With the help of the sector nonlinearity approach (Tanaka and Wang, 2004), the nonlinear dynamics of AGVs is exactly represented using TS fuzzy modeling. Then, a TS fuzzy model-based fault detector can be designed using the direct Lyapunov stability method. However, the TS fuzzy form of AGVs presents the well-known challenge in dealing with unmeasured premise variables, which still remains an open research topic in TS fuzzy observer design framework (Bergsten et al., 2002; Nguyen et al., 2021b; Nguyen et al., 2021; Pan et al., 2020).

This paper presents a new approach to deal with unmeasured premise variables in TS fuzzy actuator fault detector design for AGVs. To this end, the nonlinear model of AGVs is exactly represented in a specific TS fuzzy form with nonlinear consequents, which will be called here N-TS fuzzy model (Dong et al., 2010; Coutinho et al., 2020). This TS fuzzy form allows isolating all unmeasured premise variables in the local nonlinear consequent which enables a more effective way to exploit the differential mean value theorem (Phanomchoeng and Rajamani, 2010) for fuzzy actuator fault detector design. Using Lyapunov stability method, sufficient conditions are derived in

⋆ This work is supported in part by the French Ministry of Higher Education and Research, in part by the National Center for Scientific Research (CNRS), in part by the Hauts-de-France Region under the project ELSAT 2020, in part by the National Natural Science Foundation of China under Grant 61463001, in part by the Major Special Project of North Minzu University under Grant ZDZX201902, in part by the Third Batch of Ningxia Youth Talents Supporting Program under Grant TJGC2018097, in part by the Advanced Intelligent Perception and Control Technology Innovative Team of Ningxia.


10.1016/j.ifacol.2021.10.033

the form of linear matrix inequalities which can be effectively solved with available numerical solvers. Moreover, to improve the fault sensibility, a mixed $H_\infty/H_-$ performance is taken into account in the design procedure within a finite-frequency domain. An illustrative simulation has been performed to show the usefulness of the proposed TS fuzzy fault detection observer in detecting some small-amplitude steering faults.

*Notation.* The set of nonnegative integers is denoted by $\mathbb{Z}_+$ and $\mathcal{I}_r = \{1, 2, \dots, r\} \subset \mathbb{Z}_+$. For $i \in \mathcal{I}_r$, we denote $\sigma_r(i) = [0, \dots, 0, \overbrace{1}^{i\text{th}}, 0, \dots, 0]^\top \in \mathbb{R}^r$ a vector of the canonical basis of $\mathbb{R}^r$. For a vector $x$, $x_i$ denotes its $i$th entry. For two vectors $x, y \in \mathbb{R}^n$, the convex hull of these vectors is denoted as $\mathrm{co}(x, y) = \{\lambda x + (1-\lambda)y : \lambda \in [0, 1]\}$. For a matrix $X$, $X^\top$ denotes its transpose, $X \succ 0$ means $X$ is symmetric positive definite, and $\mathrm{He}X = X + X^\top$. $\mathrm{diag}(X_1, X_2)$ denotes a block-diagonal matrix composed of $X_1$, $X_2$. $I$ denotes the identity matrix of appropriate dimension. In block matrices, the symbol $\star$ stands for the terms deduced by symmetry. Arguments are omitted when their meaning is clear.

## 2. VEHICLE MODELING

This section present the vehicle modeling for observer-based fault detection purposes. The vehicle nomenclature is given in Table 1

Table 1. Parameter Parameters.

| | Description | Value |
|---|---|---|
| $M_v$ | Vehicle mass | 1476 [kg] |
| $l_f$ | Distance from gravity center to front axle | 1.13 [m] |
| $l_r$ | Distance from gravity center to rear axle | 1.49 [m] |
| $I_e$ | Effective longitudinal inertia | 442.8 [kgm$^2$] |
| $I_z$ | Vehicle yaw moment of inertia | 1810 [kgm$^2$] |
| $C_f$ | Front cornering stiffness | 57000 [N/rad] |
| $C_r$ | Rear cornering stiffness | 59000 [N/rad] |
| $C_x$ | Longitudinal aerodynamic drag coefficient | 0.35 [–] |
| $C_y$ | Lateral aerodynamic drag coefficient | 0.45 [–] |

### 2.1 Nonlinear Vehicle Model

We adopt the following 2-DOF nonlinear vehicle model to represent the vehicle dynamics in the horizontal plane (Swaroop and Yoon, 1999; Nguyen et al., 2021a):

$$\begin{aligned} \dot{v}_x &= \frac{T_{eng} - C_x v_x^2}{I_e} + v_y r \\ \dot{v}_y &= \frac{F_{yf} + F_{yr} - C_y v_y^2}{M_v} - v_x r \\ \dot{r} &= \frac{l_f F_{yf} - l_r F_{yr}}{I_z} \end{aligned} \tag{1}$$

where $v_x$ is the vehicle longitudinal speed, $v_y$ is the lateral speed, $r$ is the vehicle yaw rate, and $T_{eng}$ represents the torque input for the vehicle longitudinal dynamics (Rajamani, 2012). We consider normal driving situations with small angle assumption (Rajamani, 2012; Nguyen et al., 2017). Moreover, the lateral tire forces are proportional to the slip angles of each axle. Hence, the cornering forces at the front tires $F_{yf}$ and at the rear tires $F_{yr}$ can be approximated by

$$\begin{aligned} F_{yf} &= 2C_f \left(\delta - \frac{v_y + l_f r}{v_x}\right), \\ F_{yr} &= 2C_r \left(\frac{l_r r - v_y}{v_x}\right), \end{aligned} \tag{2}$$

where $\delta$ is the front wheel steering angle.

From (1) and (2), the nonlinear vehicle dynamics can be obtained as follows:

$$\dot{x} = A_v(x)x + B_v u, \tag{3}$$

where $x = [v_x \ v_y \ r]^\top$ is the vehicle state vector, $u = [T_{eng} \ \delta]^\top$ is the control input, and

$$A_v(x) = \begin{bmatrix} a_{11} & 0 & v_y \\ 0 & a_{22} & a_{23} \\ 0 & a_{32} & a_{33} \end{bmatrix}, \quad B_v = \begin{bmatrix} b_{11} & 0 \\ 0 & b_{22} \\ 0 & b_{32} \end{bmatrix},$$

with

$$\begin{aligned} a_{11} &= -\frac{C_x v_x}{I_e}, & b_{11} &= \frac{1}{I_e} \\ a_{22} &= -\frac{2(C_f + C_r)}{M_v v_x} - \frac{C_y v_y}{M_v}, & a_{23} &= \frac{2(C_r l_r - C_f l_f)}{M_v v_x} - v_x \\ a_{32} &= \frac{2(l_r C_r - C_f l_f)}{I_z v_x}, & a_{33} &= -\frac{2(C_f l_f^2 + C_r l_r^2)}{I_z v_x} \\ b_{22} &= \frac{2C_f}{M_v}, & b_{32} &= \frac{2 l_f C_f}{I_z}. \end{aligned}$$

Furthermore, we assume that the vehicle speed $v_x$ and the yaw rate $r$ can be measured whereas the information of the lateral speed $v_y$ is not available due to cost reasons. Hence, the output equation of system (3) is given by

$$y = Cx, \quad C = \begin{bmatrix} 1 & 0 & 0 \\ 0 & 0 & 1 \end{bmatrix}.$$

### 2.2 Vehicle Fuzzy Modeling for Nonlinear Observer Design

Taking into account the physical limitations during normal driving conditions (Nguyen et al., 2017), the compact set of the vehicle state is defined as

$$\mathscr{S}_x = \left\{ v_x \in [\underline{v}_x, \overline{v}_x], \ v_y \in [\underline{v}_y, \overline{v}_y], \ r \in [\underline{r}, \overline{r}] \right\}, \tag{4}$$

where $\underline{v}_x = 5$ [m/s], $\overline{v}_x = 30$ [m/s], $\underline{v}_y = -1.5$ [m/s], $\overline{v}_y = 1.5$ [m/s], $\underline{r} = -0.55$ [rad/s] and $\overline{r} = 0.55$ [rad/s]. It can be seen that the vehicle system (3) has three nonlinearities (or premise variables), *i.e.*, $v_x$, $\frac{1}{v_x}$ and $v_y$. Therefore, with the sector nonlinearity approach (Tanaka and Wang, 2004), a classical eight-rule TS fuzzy model of the nonlinear vehicle dynamics (3) can be easily derived, which is not given here for brevity. Up to now, such a TS fuzzy representation has been widely used for vehicle dynamics estimation (Zhang et al., 2016). However, this classical TS fuzzy form leads to both theoretical and practical difficulties for vehicle observer design due to the presence of unmeasured premise variables involved in the membership functions (MFs) (Nguyen et al., 2021a). To overcome this major drawback, inspired by the N-TS fuzzy modeling (Coutinho et al., 2020), we reformulate the vehicle system (3) in the following form:

$$\dot{x} = A_v(\xi)x + B_v u + g_v(\xi) + G_v \phi(x) \tag{5}$$

where $\phi(x) = v_y^2$, and

$$A_v(\xi)=\begin{bmatrix}0 & r & 0\\ 0 & -\dfrac{2(C_f+C_r)}{M_v v_x} & 0\\ 0 & \dfrac{2(l_rC_r-C_fl_f)}{I_z v_x} & 0\end{bmatrix},\qquad \xi=\begin{bmatrix}\dfrac{1}{v_x}\\ r\end{bmatrix},$$

$$g_v(\xi)=\begin{bmatrix}-\dfrac{C_x v_x^2}{I_e}\\ \dfrac{2(C_rl_r-C_fl_f)r}{M_v v_x}-v_x r\\ -\dfrac{2(C_fl_f^2+C_rl_r^2)r}{I_z v_x}\end{bmatrix},\quad G_v=\begin{bmatrix}0\\ -\dfrac{C_y}{M_v}\\ 0\end{bmatrix}.$$

Using Euler discretization method, with the sampling time $T_s = 0.01$ [s], the discrete-time counterpart of system (5) can be obtained as

$$\begin{aligned}x_{k+1} &= A(\xi_k)x_k + Bu_k + g(\xi_k) + G\phi(x_k),\\ y_k &= Cx_k,\end{aligned} \tag{6}$$

where

$$\begin{aligned}A(\xi_k) &= T_sA_v(\xi_k)+I, \quad G = T_sG_v,\\ g(\xi_k) &= T_sg_v(\xi_k), \qquad\quad B = T_sB_v.\end{aligned}$$

Using the sector nonlinearity approach (Tanaka and Wang, 2004) with the premise vector $\xi \in \mathbb{R}^2$, the following four-rule TS model of system (6) can be easily derived:

$$\begin{aligned}x_{k+1} &= A(h)x_k + Bu_k + g(\xi_k) + G\phi(x_k),\\ y_k &= Cx_k,\end{aligned} \tag{7}$$

where $A(h)=\sum_{i=1}^{4} h_i(\xi_k)A_i$. The MFs satisfy the following convex sum property:

$$0 \le h_i(\xi_k) \le 1, \quad \sum_{i=1}^{4} h_i(\xi_k) = 1. \tag{8}$$

The details on the local matrices $A_i$ and the MFs $h_i(\xi_k)$, for $i \in \mathcal{I}_4$, are not given here for brevity. Let $\Omega$ be the set of MFs satisfying (8), i.e., $h = [h_1(\xi),\ h_2(\xi),\ h_3(\xi),\ h_4(\xi)]^\top \in \Omega$.

This paper aims at detecting the presence of actuator faults for AGVs. For this purpose, we consider model (7) with disturbance $d_k$ and fault $f_k$ as follows:

$$\begin{aligned}x_{k+1} &= A(h)x_k + Bu_k + g(\xi_k) + G\phi(x_k) + Dd_k + Ff_k\\ y_k &= Cx_k,\end{aligned} \tag{9}$$

Assume that $d_k$ and $f_k$ are energy-bounded, whose frequency ranges are known *a priori*. Without loss of generality, in this paper we consider a low-frequency domain, i.e., $|\omega| < \vartheta_l$, which covers most of the practical situations within vehicle fault detection context.

## 3. FAULT DETECTION PROBLEM FORMULATION

For fault detection purposes, we consider the following observer structure:

$$\begin{aligned}z_{k+1} &= N(h)z_k + L(h)y_k + Mg(\xi_k) + MBu_k + MG\phi(\hat{x}_k),\\ \hat{x}_k &= z_k - Ey_k,\\ \hat{y}_k &= C\hat{x}_k,\end{aligned} \tag{10}$$

where $z_k$ is the observer state variable, $\hat{x}_k$ is the estimate of $x_k$. The MFs-dependent matrices $N(h)$, $L(h)$, $M$ and $E$ are to be designed such that

$$\begin{aligned}[N(h)\ \ L(h)] &= \sum_{i=1}^{4} h_i(\xi_k)\,[N_i\ \ L_i],\\ M &= I + EC.\end{aligned} \tag{11}$$

With the definition of the state estimation error $e_k = x_k - \hat{x}_k$ and the residual signal $r_k = y_k - \hat{y}_k$, it follows form (10) and (11) that

$$e_k = Mx_k - z_k, \quad r_k = Ce_k. \tag{12}$$

Therefore, under the condition

$$MA(h) - N(h)M - L(h)C = 0, \tag{13}$$

the estimation error dynamics can be defined from (9), (10) and (12) as

$$\begin{aligned}e_{k+1} &= N(h)e_k + \bar{D}\hat{d}_k + \bar{F}f_k + MG\Delta_\phi,\\ r_k &= Ce_k,\end{aligned} \tag{14}$$

where

$$\begin{aligned}\hat{d}_k &= \left[d_k^\top\ \ d_{k+1}^\top\right]^\top, \quad \Delta_\phi = \phi(x_k) - \phi(\hat{x}_k),\\ \bar{F} &= MF, \qquad\qquad \bar{D} = MD.\end{aligned}$$

The mismatching term $\Delta_\phi$ in (14) raises major challenge in observer design (Bergsten et al., 2002; Pan et al., 2020). To effectively deal with this term and guarantee an asymptotic estimation error convergence, the term $\Delta_\phi = \phi(x_k) - \phi(\hat{x}_k)$ can be reformulated as a function of the estimation error $e_k$ with the following lemma.

*Lemma 1.* (Phanomchoeng and Rajamani, 2010) Let $g(x) : \mathbb{R}^{n_x} \to \mathbb{R}^q$ and $a, b \in \mathbb{R}^{n_x}$. If $g(x)$ is differentiable on $\mathrm{co}(a, b)$, then there exist constant vectors $c_i \in \mathrm{co}(a, b)$, $c_i \neq a$, $c_i \neq b$, for $\forall i \in \mathcal{I}_q$, such that

$$g(a) - g(b) = \left(\sum_{i=1}^{q}\sum_{j=1}^{n_x} \sigma_q(i)\sigma_{n_x}^\top(j)\frac{\partial g_i}{\partial x_j}(c_i)\right)(a - b).$$

Applying Lemma 1 to $\phi(x_k)$, it follows that there exist $\nu_i \in \mathrm{co}(x_k, \hat{x}_k)$, for $i \in \mathcal{I}_1$, such that

$$\begin{aligned}\Delta_\phi &= \left(\sum_{i=1}^{1}\sum_{j=1}^{3} \sigma_1(i)\sigma_3^\top(j)\frac{\partial \phi_i}{\partial x_j}(\nu_i)\right)(x_k - \hat{x}_k),\\ &= \underbrace{[\rho_{11}\ \ \rho_{12}\ \ \rho_{13}]}_{\rho} e_k.\end{aligned} \tag{15}$$

where $\rho_{ij} = \frac{\partial \phi_i}{\partial x_j}(\nu_i)$, for $\forall (i, j) \in \mathcal{I}_1 \times \mathcal{I}_3$. Since $x \in \mathscr{S}_x$ as defined in (4), the parameter $\rho$ belongs to a bounded convex set $\mathscr{S}_\phi$, whose vertices are given by

$$\mathscr{V}_\phi = \{\rho = [\rho_{11}\ \ \rho_{12}\ \ \rho_{13}] :\ \rho_{ij} \in [\underline{\rho}_{ij}, \overline{\rho}_{ij}]\}.$$

From (14) and (15), the error dynamics is rewritten as

$$\begin{aligned}e_{k+1} &= \mathscr{N}(h, \rho)e_k + \bar{D}\hat{d}_k + \bar{F}f_k,\\ r_k &= Ce_k,\end{aligned} \tag{16}$$

where $\mathscr{N}(h, \rho) = \sum_{i=1}^{4} h_i(\xi_k)\mathscr{N}_i(\rho_{lj})$ and

$$\mathscr{N}_i(\rho_{lj}) = N_i + MG\sum_{l=1}^{1}\sum_{j=1}^{3} \sigma_1(l)\sigma_3^\top(j)\rho_{lj}.$$

To obtain a satisfactory fault detection performance for AGVs, we have to ensure the asymptotic stability of the estimation error dynamics (16) such that the residual output is as sensible as possible to the actuator fault signal $f_k$ and as robust as possible to the disturbance signal $\hat{d}_k$.

## 4. LOW-FREQUENCY FAULT DETECTION OBSERVER DESIGN

We first recall the following lemma which will be used to develop the main results of this paper.

*Lemma 2.* (Chibani et al., 2017) Consider the system

$$\begin{aligned} e_{k+1} &= \mathcal{A}e_k + \mathcal{B}\eta_k \\ r_k &= \mathcal{C}e_k + \mathcal{D}\eta_k \end{aligned} \tag{17}$$

1) Given a positive scalar $\gamma$. System (17) satisfies the $H_\infty$ performance index $\|r_k\|_2 < \gamma\|\eta_k\|_2$ in a low-frequency domain, i.e., $|\omega| < \vartheta_l$, if there exist MFs-dependent matrices $P(h) = \sum_{i=1}^{r} h_i(\xi_k)P_i$, $P(h_+) = \sum_{i=1}^{r} h_i(\xi_{k+1})P_i$, and matrix $Q > 0$ such that
$$\Phi^\top \Xi \Phi + \Psi^\top \Pi_d \Psi < 0. \tag{18}$$
2) Given a positive scalar $\beta$. System (17) satisfies the $H_-$ performance index $\|r_k\|_2 > \beta\|\eta_k\|_2$ in a low-frequency domain, i.e., $|\omega| < \vartheta_l$, if there exist MFs-dependent matrices $P(h) = \sum_{i=1}^{r} h_i(\xi_k)P_i$, $P(h_+) = \sum_{i=1}^{r} h_i(\xi_{k+1})P_i$, and matrix $Q > 0$ such that
$$\Phi^\top \Xi \Phi + \Psi^\top \Pi_f \Psi < 0. \tag{19}$$

The block-matrices involved in conditions (18) and (19) are given by

$$\Pi_d = \begin{bmatrix} I & 0 \\ 0 & -\gamma^2 I \end{bmatrix}, \quad \Phi = \begin{bmatrix} \mathcal{A} & \mathcal{B} \\ I & 0 \end{bmatrix}, \quad \Psi = \begin{bmatrix} \mathcal{C} & \mathcal{D} \\ 0 & I \end{bmatrix},$$
$$\Pi_f = \begin{bmatrix} -I & 0 \\ 0 & \beta^2 I \end{bmatrix}, \quad \Xi = \begin{bmatrix} -P(h_+) & Q \\ Q & P(h) - 2\cos(\vartheta_l)Q \end{bmatrix}.$$

### *4.1 Internal Stability Condition*

This section presents sufficient conditions to ensure the internal stability of the state estimation error system (16).

*Theorem 1.* Consider the observer structure (10) under conditions (11) and (13). The estimation error system (16) is stable if there exist MFs-dependent matrix $P_s(h) > 0$, $N(h)$, and matrices $R$, $M$, $E$, such that

$$\begin{bmatrix} P_s(h) & * \\ R\mathcal{N}(h,\rho) & R + R^\top - P_s(h_+) \end{bmatrix} > 0, \tag{20}$$

for $h, h_+ \in \Omega$, $\rho \in \mathscr{S}_\phi$.

**Proof.** For internal stability analysis, we consider $d_k = 0$ and $f_k = 0$. Then, the error system (16) becomes

$$e_{k+1} = \mathcal{N}(h,\rho)e_k. \tag{21}$$

Pre- and postmultiplying (20) with $[I \ -\mathcal{N}(h,\rho)]^\top$ and its transpose, we obtain

$$\mathcal{N}(h,\rho)^\top P_s(h_+)\mathcal{N}(h,\rho) - P_s(h) < 0. \tag{22}$$

For the asymptotic stability analysis of the error dynamics (21), we consider the fuzzy Lyapunov function candidate

$$V_s(e_k) = e_k^\top P_s(h) e_k, \tag{23}$$

with $P_s(h) > 0$. The variation of the fuzzy Lyapunov function (23) along the trajectory of system (21) is defined as follows:

$$\begin{aligned} \Delta V_s &= V_s(e_{k+1}) - V_s(e_k) \\ &= e_k^\top \left( \mathcal{N}(h,\rho)^\top P_s(h_+)\mathcal{N}(h,\rho) - P_s(h) \right) e_k. \end{aligned} \tag{24}$$

It follows from (22) and (24) that $\Delta V_s < 0$, for $\forall e_k \neq 0$. This concludes the proof.

### *4.2 Disturbance Attenuation Condition*

This section presents sufficient conditions to guarantee an $H_\infty$ performance with respect to disturbances in low-frequency domain. Hence, in this case we consider the estimation error dynamics (16) with $f_k = 0$, i.e.,

$$\begin{aligned} e_{k+1} &= \mathcal{N}(h,\rho)e_k + \bar{D}\bar{d}_k, \\ r_k &= Ce_k, \end{aligned} \tag{25}$$

where $\bar{d}_k$ is of low frequency, i.e., $|\omega_d| < \vartheta_{d_l}$.

*Theorem 2.* Given a scalar $\alpha_d$, the system (25) has a low-frequency $H_\infty$ performance index $\gamma$, if there exist MFs-dependent matrices $P_d(h)$, $N(h)$, $L(h)$ and matrices $Q_d > 0$, $R$, $M$, $E$ under the conditions of (11) and (13) such that the following condition is satisfied for $h, h_+ \in \Omega$, $\rho \in \mathscr{S}_\phi$

$$\begin{bmatrix} \Sigma_{11} & * & * \\ \Sigma_{21} & -\gamma^2 I & * \\ \Sigma_{31} & R\bar{D} & -P_d(h_+) - R - R^\top \end{bmatrix} < 0, \tag{26}$$

where

$$\begin{aligned} \Sigma_{11} &= \mathrm{He}(\alpha_d R\mathcal{N}(h,\rho)) + P_d(h) - 2\cos(\vartheta_{d_l})Q_d + C^\top C, \\ \Sigma_{21} &= \alpha_d(R\bar{D})^\top, \\ \Sigma_{31} &= R\mathcal{N}(h,\rho) + Q_d - \alpha_d R^\top. \end{aligned}$$

**Proof.** Pre- and postmultiplying condition (26) with

$$\begin{bmatrix} I & 0 & \mathcal{N}(h,\rho)^\top \\ 0 & I & \bar{D}^\top \end{bmatrix}$$

and its transpose, we obtain

$$\Phi_d^\top \Xi \Phi_d + \Psi_d^\top \Pi_d \Psi_d < 0, \tag{27}$$

where

$$\Phi_d = \begin{bmatrix} \mathcal{N}(h,\rho) & \bar{D} \\ I & 0 \end{bmatrix}, \quad \Psi_d = \begin{bmatrix} C & 0 \\ 0 & I \end{bmatrix}.$$

According to Lemma 2, inequality (27) implies that an $H_\infty-$gain performance of $\gamma$ is guaranteed for the error system (25) in low-frequency domain. This concludes the proof.

### *4.3 Fault Sensitivity Condition*

This section presents sufficient conditions to analyze the fault sensitivity performance in finite-frequency domain. Hence, we consider the error system (16) with $d_k = 0$, i.e.,

$$\begin{aligned} e_{k+1} &= \mathcal{N}(h,\rho)e_k + \bar{F}f_k, \\ r_k &= Ce_k, \end{aligned} \tag{28}$$

where $f_k$ is of low frequency, i.e., $|\omega_f| < \vartheta_{f_l}$.

*Theorem 3.* Given a scalar $\alpha_f$ and a matrix $V \in \mathbb{R}^{n_f \times n_x}$, the error system (28) has a low-frequency $H_-$ performance index $\beta$, if there exist MFs-dependent matrices $P_f(h)$, $N(h)$, $L(h)$ and matrices $Q_f > 0$, $R$, $M$, $E$, such that the following condition is satisfied for $h, h_+ \in \Omega$, $\rho \in \mathscr{S}_\phi$

$$\begin{bmatrix} \Delta_{11} & * & * \\ \Delta_{21} & \mathrm{He}(VRMF) + \beta^2 I & * \\ \Delta_{31} & -(VR)^\top + RMF & -P_f(h_+) - R - R^\top \end{bmatrix} < 0, \tag{29}$$

where

$$\begin{aligned} \Delta_{11} &= \mathrm{He}(\alpha_f R\mathcal{N}(h,\rho)) + P_f(h) - 2\cos(\vartheta_{f_l})Q_f - C^\top C, \\ \Delta_{21} &= \alpha_f(RMF)^\top + VR\mathcal{N}(h,\rho), \\ \Delta_{31} &= R\mathcal{N}(h,\rho) + Q_f - \alpha_f R^\top. \end{aligned}$$

**Proof.** Pre- and postmultiplying condition (29) with

$$\begin{bmatrix} I & 0 & \mathcal{N}(h,\rho)^\top \\ 0 & I & \bar{F}^\top \end{bmatrix}$$

and its transpose, we obtain

$$\Phi_f^\top \Xi \Phi_f + \Psi_f^\top \Pi_f \Psi_f < 0, \tag{30}$$

where

$$\Phi_f = \begin{bmatrix} \mathscr{N}(h,\rho) & \bar{F} \\ I & 0 \end{bmatrix}, \quad \Psi_f = \begin{bmatrix} C & 0 \\ 0 & I \end{bmatrix}.$$

According to Lemma 2, inequality (30) implies that the system (28) has an $H_-$ fault sensitivity performance in low-frequency domain. This concludes the proof.

### 4.4 Finite-Frequency Fault Detection Observer Design

Due to the involved nonlinear matrix equality (11), the nonlinear matrix inequalities and their MF-dependency, Theorems 1∼3 cannot be directly solved for finite-frequency fault detection observer design. Based on the results of these theorems, we derive hereafter tractable conditions to design fault detection observer (10) for system (9).

*Theorem 4.* Given scalars $\alpha_d$, $\alpha_f$ and a matrix $V$, the estimation error system (16) is stable while verifying a finite-frequency $H_\infty$ performance index $\gamma$ as well as a finite-frequency $H_-$ performance index $\beta$, if there exist a scalar $\beta > 0$ and matrices $P_{s_i} > 0$, $P_{d_i}$, $P_{f_i}$, $Q_d > 0$, $Q_f > 0$, $R$, $S$, $W_i$, such that

$$\begin{bmatrix} \Gamma_{11} & * & * & * \\ \Gamma_{21} & -\gamma^2 I & * & * \\ 0 & 0 & -\gamma^2 I & * \\ \Gamma_{41} & \Gamma_{42} & 0 & -P_{d_k} - R - R^\top \end{bmatrix} < 0, \tag{31}$$

$$\begin{bmatrix} \Lambda_{11} & * & * \\ \Lambda_{21} & \Lambda_{22} & * \\ \Lambda_{31} & \Lambda_{32} & -P_{f_k} - R - R^\top \end{bmatrix} < 0, \tag{32}$$

$$\begin{bmatrix} P_{s_i} & * \\ (R+SC)\mathscr{A}_i(\rho_{lj}) - W_i C & R + R^\top - P_{s_k} \end{bmatrix} > 0, \tag{33}$$

for $i, k \in \mathcal{I}_r$ and $\rho_{lj} \in \mathscr{V}_\phi$, $l \in \mathcal{I}_{n_\phi}$, $j \in \mathcal{I}_{n_x}$, where

$$\mathscr{A}_i(\rho_{lj}) = A_i + G_i \sum_{l=1}^{n_\phi} \sum_{j=1}^{n_x} \sigma_{n_\phi}(l) \sigma_{n_x}^\top(j) \rho_{lj},$$

$$\Gamma_{11} = P_{d_i} + C^\top C + \alpha_d \mathrm{He}((R+SC)\mathscr{A}_i(\rho_{lj}) - W_i C) - 2\cos(\vartheta_{d_l}) Q_d,$$

$$\Gamma_{21} = \alpha_d ((R+SC)D)^\top,$$

$$\Gamma_{41} = (R+SC)\mathscr{A}_i(\rho_{lj}) - W_i C + Q_d - \alpha_d R^\top,$$

$$\Gamma_{42} = (R+SC)D,$$

$$\Lambda_{11} = P_{f_i} - C^\top C + \alpha_f \mathrm{He}((R+SC)\mathscr{A}_i(\rho_{lj}) - W_i C), - 2\cos(\vartheta_{f_l}) Q_f,$$

$$\Lambda_{21} = \alpha_f ((R+SC)F)^\top + V(R+SC)\mathscr{A}_i(\rho_{lj}) - V W_i C,$$

$$\Lambda_{22} = \mathrm{He}(V(R+SC)F) + \beta^2 I,$$

$$\Lambda_{31} = (R+SC)\mathscr{A}_i(\rho_{lj}) - W_i C + Q_f - \alpha_f R^\top,$$

$$\Lambda_{32} = -(VR)^\top + (R+SC)F.$$

**Proof.** Let us define

$$H_i = L_i + N_i F. \tag{34}$$

Then, from (11), (13) and (34), it follows that

$$N_i = M A_i - H_i C. \tag{35}$$

According to the results of Theorems 1∼3, we substitute (34) and (35) into conditions (26), (29) and (20) while considering

$$S = RE, \tag{36}$$

$$W_i = R H_i, \tag{37}$$

then we can obtain conditions (31), (32) and (33). This concludes the proof.

Table 2. Finite-Frequency Fault Detection Observer Design Algorithm

| **Design Procedure** | |
|---|---|
| Step 1 | Solve conditions in Theorem 4 to get $R$, $S$, $W_i$, $i \in \mathcal{I}_r$. |
| Step 2 | Compute observer matrix $E$ from (36) as $E = R^{-1}S$. |
| Step 3 | Compute $H_i$ from (37) as $H_i = R^{-1}W_i$, $i \in \mathcal{I}_r$. |
| Step 4 | Compute observer matrix $M$ from (11). |
| Step 5 | Compute observer matrices $N_i$, $i \in \mathcal{I}_r$, from (35). |
| Step 6 | Compute observer matrices $L_i$, $i \in \mathcal{I}_r$, from (34). |

To increase the fault detection sensitivity, the following optimization problem can be performed.

$$\begin{aligned} &\max \quad \beta \\ &\text{s.t.} \quad (31),\ (32),\ (33). \end{aligned}$$

The algorithm for finite-frequency fault detection observer design of autonomous vehicles is summarized in Table 2.

### 4.5 Residual Evaluation and Threshold Setting

To detect whether a fault occurs, an evaluation function and the corresponding threshold are necessary after determining the finite-frequency TS fuzzy observer. To this end, the following root mean square (RMS) function of the residual is considered as an evaluation function (Zhou et al., 2019):

$$J_{RMS}(k) = ||r_k||_{RMS} = \sqrt{\frac{1}{\Delta T} \sum_{k=1}^{\Delta T} ||r_{t+k}||^2}$$

where $\Delta T$ is a time window to be determined based on applications. Then, the threshold is chosen as

$$J_{th}(k) = \sup_{f_k = 0} ||r_k||_{RMS}.$$

Finally, the fault detection logic can be defined as

$$\begin{cases} J_{RMS} < J_{th}(k) & \Rightarrow \quad \text{Fault free} \\ J_{RMS} \geq J_{th}(k) & \Rightarrow \quad \text{Fault alarm.} \end{cases}$$

## 5. SIMULATION RESULTS

This section presents numerical illustrations obtained with the proposed fault detection observer design. Note that all LMI-based optimizations are performed with YALMIP toolbox using SDPT3 solver. An observer solution can be obtained while solving the conditions in Theorem 4 with $\gamma = 0.8$, $\alpha_d = 2$, $V = F^\top$, $\alpha_f = 1$. To evaluate the fault detection performance, we consider the following initial condition for the 2-DOF vehicle model (1) and the designed TS fuzzy observer (10):

$$x_k = [-5 \ 1 \ 0]^\top, \quad z_k = [0 \ 0 \ 0]^\top.$$

The moving time window is chosen as $\Delta T = 40$. We assume that the disturbance signal of the system is defined as

$$d_k = 0.1 \sin(-0.1\pi t).$$

The following steering fault scenario is considered for numerical illustrations:

$$f(k) = \begin{cases} 0.5 + 0.1\sin(-0.1\pi t), & \text{if } t > 5 \\ 0, & \text{otherwise.} \end{cases}$$

Fig. 1 depicts the simulation result obtained with the proposed finite-frequency fault detection algorithm. We can see that the proposed TS fuzzy observer-based approach has a high sensitivity for fault detection, which is useful to detect some minor actuator faults.

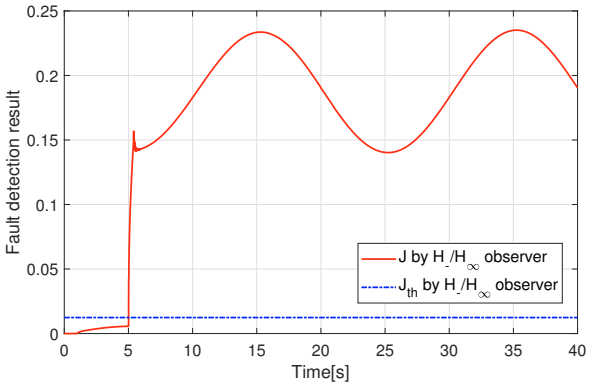


Fig. 1. Fault detection performance obtained with the proposed TS fuzzy observer-based approach.

## 6. CONCLUSIONS

A new approach has been proposed to deal with unmeasured premise variables in the design of TS fuzzy fault detection observer for AGVs represented by an 2-DOF bicycle model. We reformulate this nonlinear vehicle model in the form of a TS fuzzy system with nonlinear consequents where all the unmeasured premise variables are isolated in the consequent parts. Using the differential mean value theorem and Lyapunov stability theorem, a new fault detector can be designed for steering actuator fault. Finite-frequency specifications are taken into account in the observer design to increase the fault sensibility performance. Simulation results clearly demonstrate the effectiveness of the proposed fault detection observer design. Future works focus on reducing further the design conservatism while considering more deeply different actuator fault detection scenarios of AGVs.

## REFERENCES

Arogeti, S., Wang, D., Low, C., and Yu, M. (2012). Fault detection isolation and estimation in a vehicle steering system. *IEEE Trans. Indus. Electron.*, 59(12), 810–820.

Bergsten, P., Palm, R., and Driankov, D. (2002). Observers for Takagi-Sugeno fuzzy systems. *IEEE Trans. Syst., Man, Cybern., Part B (Cybern.)*, 32(1), 114–121.

Chibani, A., Chadli, M., Shi, P., and Braiek, N.B. (2017). Fuzzy fault detection filter design for T-S fuzzy systems in the finite-frequency domain. *IEEE Trans. Fuzzy Syst.*, 25(5), 1051–1061.

Coutinho, P., Araújo, R., Nguyen, A.T., and Palhares, R. (2020). A multiple-parameterization approach for local stabilization of constrained Takagi-Sugeno fuzzy systems with nonlinear consequents. *Inf. Sci.*, 506, 295–307.

Dong, J., Wang, Y., and Yang, G. (2010). Output feedback fuzzy controller design with local nonlinear feedback laws for discrete-time nonlinear systems. *IEEE Trans. Syst., Man, Cybern. B, Cybern.*, 40(6), 1447–1459.

Fang, Y., Min, H., Wang, W., Xu, Z., and Zhao, X. (2020). A fault detection and diagnosis system for autonomous vehicles based on hybrid approaches. *IEEE Sensors J.*, 20(16), 9359–9371. doi:10.1109/JSEN.2020.2987841.

Li, P., Nguyen, A.T., Du, H., Wang, Y., and Zhang, H. (2021). Polytopic LPV approaches for intelligent automotive systems: State of the art and future challenges. *Mech. Syst. Signal Process.*, 161, 107931.

Nguyen, A.T., Campos, V., Guerra, T.M., Pan, J., and Xie, W. (2021). Takagi-Sugeno fuzzy observer design for nonlinear descriptor systems with unmeasured premise variables and unknown inputs. *Int. J. Robust Nonlinear Control*. DOI: 10.1002/RNC.5453.

Nguyen, A.T., Dinh, T.Q., Guerra, T.M., and Pan, J. (2021a). Takagi-Sugeno fuzzy unknown input observers to estimate nonlinear dynamics of autonomous ground vehicles: Theory and real-time verification. *IEEE/ASME Trans. Mechatron.*, 1–1. doi:10.1109/TMECH.2020.3049070.

Nguyen, A.T., Pan, J., Guerra, T.M., and Wang, Z. (2021b). Avoiding unmeasured premise variables in designing unknown input observers for Takagi-Sugeno fuzzy systems. *IEEE Control Syst. Lett.*, 5(1), 79–84.

Nguyen, A.T., Taniguchi, T., Eciolaza, L., Campos, V., Palhares, R., and Sugeno, M. (2019). Fuzzy control systems: Past, present and future. *IEEE Comput. Intell. Mag.*, 14(1), 56–68.

Nguyen, A.T., Sentouh, C., and Popieul, J.C. (2017). Driver-automation cooperative approach for shared steering control under multiple system constraints: Design and experiments. *IEEE Trans. Indus. Electron.*, 64(5), 3819–3830.

Pan, J., Nguyen, A.T., Guerra, T.M., and Ichalal, D. (2020). A unified framework for asymptotic observer design of fuzzy systems with unmeasurable premise variables. *IEEE Trans. Fuzzy Syst.*, 1–1. DOI: 10.1109/TFUZZ.2020.3009737.

Phanomchoeng, G. and Rajamani, R. (2010). The bounded Jacobian approach to nonlinear observer design. In *American Control Conf.*, 6083–6088. IEEE.

Rajamani, R. (2012). *Vehicle Dynamics and Control*. Springer US.

Swaroop, D. and Yoon, S. (1999). The design of a controller for a following vehicle in an emergency lane change maneuver. California PATH Working Paper UCB-ITS-PWP-99-3, University of California.

Tanaka, K. and Wang, H. (2004). *Fuzzy Control Systems Design and Analysis: a Linear Matrix Inequality Approach*. NY: Wiley-Interscience.

Zhang, B., Du, H., Lam, J., Zhang, N., and Li, W. (2016). A novel observer design for simultaneous estimation of vehicle steering angle and sideslip angle. *IEEE Trans. Indus. Electron.*, 63(7), 4357–4366.

Zhou, M., Cao, Z., Zhou, M., and Wang, J. (2019). Finite-frequency $H_-/H_\infty$ fault detection for discrete-time T-S fuzzy systems with unmeasurable premise variables. *IEEE Trans. Cybern.*, 1–10.